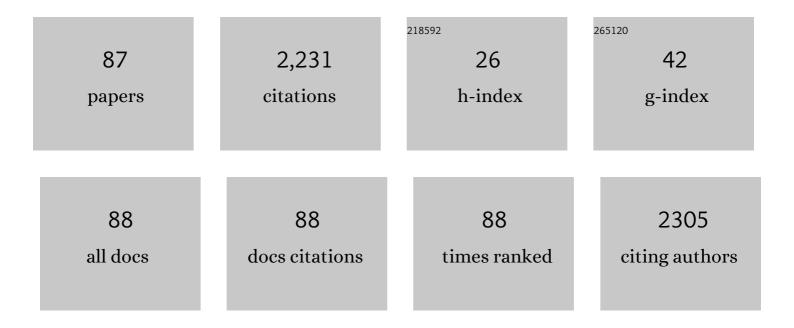
Serena Esposito

List of Publications by Year in descending order

Source: https://exaly.com/author-pdf/1992569/publications.pdf Version: 2024-02-01



#	Article	IF	CITATIONS
1	Silica Meets Tannic Acid: Designing Green Nanoplatforms for Environment Preservation. Molecules, 2022, 27, 1944.	1.7	10
2	Magnetic clustering of weakly interacting Ni-ions in Ni-exchanged zeolites. Microporous and Mesoporous Materials, 2022, 335, 111786.	2.2	1
3	Removal of sulfanilamide by tailor-made magnetic metal-ceramic nanocomposite adsorbents. Journal of Environmental Management, 2022, 310, 114701.	3.8	12
4	Ultra-fast high-temperature sintering (UHS) of Ce0.2Zr0.2Y0.2Gd0.2La0.2O2â^`î´ fluorite-structured entropy-stabilized oxide (F-ESO). Scripta Materialia, 2022, 214, 114655.	2.6	26
5	The role of metallic and acid sites of Ru-Nb-Si catalysts in the transformation of levulinic acid to Î ³ -valerolactone. Applied Catalysis B: Environmental, 2022, 310, 121340.	10.8	11
6	Solar driven photocatalysis using iron and chromium doped TiO2 coupled to moving bed biofilm process for olive mill wastewater treatment. Chemical Engineering Journal, 2022, 450, 138107.	6.6	30
7	Flame Pyrolysis Synthesis of Mixed Oxides for Glycerol Steam Reforming. Materials, 2021, 14, 652.	1.3	4
8	Effective Inclusion of Sizable Amounts of Mo within TiO ₂ Nanoparticles Can Be Obtained by Reverse Micelle Sol–Gel Synthesis. ACS Omega, 2021, 6, 5379-5388.	1.6	16
9	New Insights in the Production of Simulated Moon Agglutinates: the Use of Natural Zeolite-Bearing Rocks. ACS Earth and Space Chemistry, 2021, 5, 1631-1646.	1.2	6
10	Visible Light-Driven Photocatalytic Activity and Kinetics of Fe-Doped TiO2 Prepared by a Three-Block Copolymer Templating Approach. Materials, 2021, 14, 3105.	1.3	17
11	Reverse Micelle Strategy for the Synthesis of MnO _{<i>x</i>} –TiO ₂ Active Catalysts for NH ₃ -Selective Catalytic Reduction of NO _{<i>x</i>} at Both Low Temperature and Low Mn Content. ACS Omega, 2021, 6, 24562-24574.	1.6	12
12	Co-doped LaAlO3 perovskite oxide for NOx-assisted soot oxidation. Applied Catalysis A: General, 2020, 589, 117304.	2.2	21
13	Magnetic behavior of Ni nanoparticles and Ni2+ ions in weakly loaded zeolitic structures. Journal of Alloys and Compounds, 2020, 817, 152776.	2.8	10
14	Active and stable ceria-zirconia supported molybdenum oxide catalysts for cyclooctene epoxidation: Effect of the preparation procedure. Catalysis Today, 2020, 345, 201-212.	2.2	11
15	Effects of the Brookite Phase on the Properties of Different Nanostructured TiO ₂ Phases Photocatalytically Active Towards the Degradation of Nâ€Phenylurea. ChemistryOpen, 2020, 9, 903-912.	0.9	11
16	Muon spin relaxation study of phosphosilicate gels. Solid State Ionics, 2020, 348, 115287.	1.3	3
17	CO2 abatement and CH4 recovery at vehicle exhausts: Comparison and characterization of Ru powder and pellet catalysts. International Journal of Hydrogen Energy, 2020, 45, 8640-8648.	3.8	5
18	Hybrid organic-inorganic nanotubes effectively adsorb some organic pollutants in aqueous phase. Applied Clay Science, 2020, 186, 105449.	2.6	14

#	Article	IF	CITATIONS
19	Separation of Biological Entities from Human Blood by Using Magnetic Nanocomposites Obtained from Zeolite Precursors. Molecules, 2020, 25, 1803.	1.7	10
20	Removal of Agrochemicals from Waters by Adsorption: A Critical Comparison among Humic-Like Substances, Zeolites, Porous Oxides, and Magnetic Nanocomposites. Processes, 2020, 8, 141.	1.3	14
21	Photocatalysts for Organics Degradation. Catalysts, 2019, 9, 870.	1.6	Ο
22	Near UVâ€Irradiation of CuO _x â€Impregnated TiO ₂ Providing Active Species for H ₂ Production Through Methanol Photoreforming. ChemCatChem, 2019, 11, 4314-4326.	1.8	25
23	Simulated Moon Agglutinates Obtained from Zeolite Precursor by Means of a Low-Cost and Scalable Synthesis Method. ACS Earth and Space Chemistry, 2019, 3, 1884-1895.	1.2	9
24	Effect of RE ³⁺ on Structural Evolution of Rare-Earth Carbonates Synthesized by Facile Hydrothermal Treatment. Advances in Materials Science and Engineering, 2019, 2019, 1-10.	1.0	5
25	Self-Activating Catalyst for Glucose Hydrogenation in the Aqueous Phase under Mild Conditions. ACS Catalysis, 2019, 9, 3426-3436.	5.5	31
26	Application of Reverse Micelle Sol–Gel Synthesis for Bulk Doping and Heteroatoms Surface Enrichment in Mo-Doped TiO2 Nanoparticles. Materials, 2019, 12, 937.	1.3	21
27	"Traditional―Sol-Gel Chemistry as a Powerful Tool for the Preparation of Supported Metal and Metal Oxide Catalysts. Materials, 2019, 12, 668.	1.3	213
28	Magnetic Properties of Nanocomposites. Applied Sciences (Switzerland), 2019, 9, 212.	1.3	62
29	Magnetic metal-ceramic nanocomposites obtained from cation-exchanged zeolite by heat treatment in reducing atmosphere. Microporous and Mesoporous Materials, 2018, 268, 131-143.	2.2	24
30	Novel process to prepare magnetic metal-ceramic nanocomposites from zeolite precursor and their use as adsorbent of agrochemicals from water. Journal of Environmental Chemical Engineering, 2018, 6, 527-538.	3.3	22
31	New Insights into the Role of the Synthesis Procedure on the Performance of Co-Based Catalysts for Ethanol Steam Reforming. Topics in Catalysis, 2018, 61, 1734-1745.	1.3	15
32	The multifarious aspects of the thermal conversion of Ba-exchanged zeolite A to monoclinic celsian. Microporous and Mesoporous Materials, 2018, 256, 235-250.	2.2	12
33	Photo-activated degradation of tartrazine by H 2 O 2 as catalyzed by both bare and Fe-doped methyl-imogolite nanotubes. Catalysis Today, 2018, 304, 199-207.	2.2	38
34	Magnetic clustering of Ni2+ ions in metal-ceramic nanocomposites obtained from Ni-exchanged zeolite precursors. Ceramics International, 2018, 44, 17240-17250.	2.3	12
35	Beneficial effect of Fe addition on the catalytic activity of electrodeposited MnOx films in the water oxidation reaction. Electrochimica Acta, 2018, 284, 294-302.	2.6	13
36	A Sol–Gel Ruthenium–Niobium–Silicon Mixedâ€Oxide Bifunctional Catalyst for the Hydrogenation of Levulinic Acid in the Aqueous Phase. ChemCatChem, 2017, 9, 1476-1486.	1.8	19

#	Article	IF	CITATIONS
37	Preparation and Characterization of Magnetic and Porous Metal-Ceramic Nanocomposites from a Zeolite Precursor and Their Application for DNA Separation. Journal of Biomedical Nanotechnology, 2017, 13, 337-348.	0.5	24
38	A simple model for a complex system: Kinetics of water oxidation with the [Ru(bpy) 3] 2+ /S 2 O 8 2â~' photosystem as catalyzed by Mn 2 O 3 under different illumination conditions. Chemical Engineering Journal, 2017, 311, 143-152.	6.6	13
39	Role of pH in the Aqueous Phase Reactivity of Zerovalent Iron Nanoparticles with Acid Orange 7, a Model Molecule of Azo Dyes. Journal of Nanomaterials, 2017, 2017, 1-13.	1.5	11
40	Synthesis and Characterization of Fe-doped Aluminosilicate Nanotubes with Enhanced Electron Conductive Properties. Journal of Visualized Experiments, 2016, , .	0.2	1
41	lsomorphic substitution of aluminium by iron into single-walled alumino-silicate nanotubes: A physico-chemical insight into the structural and adsorption properties of Fe-doped imogolite. Microporous and Mesoporous Materials, 2016, 224, 229-238.	2.2	25
42	Application of highly porous materials for simazine removal from aqueous solutions. Environmental Technology (United Kingdom), 2016, 37, 2428-2434.	1.2	8
43	Reactivity of bare and Fe-doped alumino-silicate nanotubes (imogolite) with H2O2 and the azo-dye Acid Orange 7. Catalysis Today, 2016, 277, 89-96.	2.2	24
44	The role of outer surface/inner bulk BrĄ̃,nsted acidic sites in the adsorption of a large basic molecule (simazine) on H-Y zeolite. Physical Chemistry Chemical Physics, 2015, 17, 28950-28957.	1.3	10
45	Nanoparticles of CoAPO-5: synthesis and comparison with microcrystalline samples. Physical Chemistry Chemical Physics, 2015, 17, 10774-10780.	1.3	8
46	Adsorption of simazine on zeolite H-Y and sol–gel technique manufactured porous silica: A comparative study in model and natural waters. Journal of Environmental Science and Health - Part B Pesticides, Food Contaminants, and Agricultural Wastes, 2015, 50, 777-787.	0.7	6
47	Al/Fe isomorphic substitution versus Fe2O3 clusters formation in Fe-doped aluminosilicate nanotubes (imogolite). Journal of Nanoparticle Research, 2015, 17, 1.	0.8	31
48	Relationships between the water content of zeolites and their cation population. Microporous and Mesoporous Materials, 2015, 202, 36-43.	2.2	31
49	A critical role of pH in the combustion synthesis of nano-sized SrAl2O4:Eu2+, Dy3+ phosphor. Ceramics International, 2014, 40, 4697-4706.	2.3	36
50	Imogolite: An Aluminosilicate Nanotube Endowed with Low Cytotoxicity and Genotoxicity. Chemical Research in Toxicology, 2014, 27, 1142-1154.	1.7	26
51	IR spectroscopic study of the acidic properties of alumino-silicate single-walled nanotubes of the imogolite type. Catalysis Today, 2013, 218-219, 3-9.	2.2	11
52	Simazine removal from waters by adsorption on porous silicas tailored by sol–gel technique. Microporous and Mesoporous Materials, 2013, 180, 178-186.	2.2	26
53	Modes of Interaction of Simazine with the Surface of Model Amorphous Silicas in Water. Journal of Physical Chemistry C, 2013, 117, 11203-11210.	1.5	16
54	Modes of Interaction of Simazine with the Surface of Amorphous Silica in Water. Part II: Adsorption at Temperatures Higher than Ambient. Journal of Physical Chemistry C, 2013, 117, 27047-27051.	1.5	6

#	Article	IF	CITATIONS
55	CO ₂ Adsorption on Aluminosilicate Single-Walled Nanotubes of Imogolite Type. Journal of Physical Chemistry C, 2012, 116, 20417-20425.	1.5	33
56	Influence of the Devitrification Mechanism on Second Harmonic Generation Efficiency and Transparency in Ba ₂ NaNb ₅ 15 Nanostructures. Journal of Physical Chemistry C, 2012, 116, 26874-26880.	1.5	4
57	Cyclic process of simazine removal from waters by adsorption on zeolite H-Y and its regeneration by thermal treatment. Journal of Hazardous Materials, 2012, 229-230, 354-360.	6.5	29
58	Metal-ceramic composite materials from zeolite precursor. Solid State Sciences, 2012, 14, 394-400.	1.5	19
59	The role of residual Na+ and Li+ on the thermal transformation of Ba-exchangedÂzeolite A. Solid State Sciences, 2011, 13, 1143-1151.	1.5	12
60	Decontamination of waters polluted with simazine by sorption on mesoporous metal oxides. Journal of Hazardous Materials, 2011, 196, 242-247.	6.5	31
61	New insight into the preparation of copper/zirconia catalysts by sol–gel method. Applied Catalysis A: General, 2011, 403, 128-135.	2.2	28
62	Synthesis of cobalt doped silica thin film for low temperature optical gas sensor. Journal of Sol-Gel Science and Technology, 2011, 60, 388-394.	1.1	18
63	Study of the thermal transformations of Co- and Fe-exchanged zeolites A and X by "in situ―XRD under reducing atmosphere. Materials Research Bulletin, 2010, 45, 744-750.	2.7	23
64	Highly dispersed sol–gel synthesized Cu–ZrO2 materials as catalysts for oxidative steam reforming of methanol. Applied Catalysis A: General, 2010, 372, 48-57.	2.2	59
65	Parameters Expediting the Thermal Conversion of Ba-Exchanged Zeolite A to Monoclinic Celsian. Advances in Materials Science and Engineering, 2010, 2010, 1-8.	1.0	7
66	Sorption Capacity of Mesoporous Metal Oxides for the Removal of MCPA from Polluted Waters. Journal of Agricultural and Food Chemistry, 2010, 58, 5011-5016.	2.4	31
67	TPR/TPO characterization of cobalt–silicon mixed oxide nanocomposites prepared by sol–gel. Thermochimica Acta, 2008, 471, 51-54.	1.2	28
68	Effect of residual Na on the low temperature synthesis of monoclinic celsian from zeolite Ba-A. Studies in Surface Science and Catalysis, 2008, 174, 197-200.	1.5	2
69	Cobalt–silicon mixed oxide nanocomposites by modified sol–gel method. Journal of Solid State Chemistry, 2007, 180, 3341-3350.	1.4	83
70	Microwave assisted hydrothermal conversion of Ba-exchanged zeolite A into metastable paracelsian. Microporous and Mesoporous Materials, 2006, 96, 9-13.	2.2	6
71	Substitution clustering in a non-stoichiometric celsian synthesized by the thermal transformation of barium exchanged zeolite X. Journal of Solid State Chemistry, 2006, 179, 1957-1964.	1.4	14
72	Thermally induced structural and microstructural evolution of barium exchanged zeolite A to celsian. Studies in Surface Science and Catalysis, 2005, , 249-260.	1.5	4

#	Article	IF	CITATIONS
73	Films by slurry coating of nanometric YSZ (8mol% Y2O3) powders synthesized by low-temperature hydrothermal treatment. Journal of the European Ceramic Society, 2005, 25, 2017-2021.	2.8	28
74	Role of Li in the low temperature synthesis of monoclinic celsian from (Ba, Li)-exchanged zeolite-A precursor. Solid State Sciences, 2005, 7, 1406-1414.	1.5	25
75	A comparative study of the thermal transformations of Ba-exchanged zeolites A, X and LSX. Journal of the European Ceramic Society, 2004, 24, 2689-2697.	2.8	32
76	Solid state NMR study of phosphosilicate gels. Journal of Non-Crystalline Solids, 2004, 345-346, 601-604.	1.5	24
77	29Si and 27Al NMR study of the thermal transformation of barium exchanged zeolite-A to celsian. Journal of Materials Chemistry, 2003, 13, 1681.	6.7	31
78	FTIR study of the thermal transformation of barium-exchanged zeolite A to celsian. Journal of Materials Chemistry, 2002, 12, 3039-3045.	6.7	62
79	Solid state 1H NMR study, humidity sensitivity and protonic conduction of gel derived phosphosilicate glasses. Journal of Materials Chemistry, 2002, 12, 3746-3753.	6.7	27
80	Solid state 29Si and 31P NMR study of gel derived phosphosilicate glasses. Journal of Materials Chemistry, 2001, 11, 936-943.	6.7	58
81	Chemical heterogeneity in phosphosilicate gels by NMR magnetisation exchange. Dalton Transactions RSC, 2001, , 2003-2008.	2.3	9
82	Sol-Gel Synthesis of Humidity-Sensitive P2O5-SiO2 Amorphous Films. Journal of Sol-Gel Science and Technology, 2000, 17, 247-254.	1.1	71
83	Solid state 11B NMR study of glasses near the barium metaborate stoichiometry. Journal of Non-Crystalline Solids, 1999, 249, 99-105.	1.5	15
84	Structure and crystallization behavior of glasses in the BaO–B2O3–Al2O3 system. Journal of Non-Crystalline Solids, 1999, 258, 1-10.	1.5	59
85	Solid state 27Al NMR and FTIR study of lanthanum aluminosilicate glasses. Journal of Non-Crystalline Solids, 1999, 258, 11-19.	1.5	160
86	Solid state NMR and FT Raman spectroscopy of the devitrification of lithium metasilicate glass. Journal of Non-Crystalline Solids, 1998, 224, 50-56.	1.5	16
87	Ftir and dta study of lanthanum aluminosilicate glasses. Materials Chemistry and Physics, 1997, 51, 163-168.	2.0	103

6